EEET ECOLOGICAL ENGINEERING & ENVIRONMENTAL TECHNOLOGY

*Ecological Engineering & Environmental Technology*, 2026, 27(5), 413–429
https://doi.org/10.12912/27197050/220342
ISSN 2719–7050, License CC-BY 4.0

Received: 2026.03.16
Accepted: 2026.04.15
Published: 2026.05.01

# Mapping flood susceptibility and settlement exposure using random forest for spatial planning in Barru Regency

Hamman Badruttamanan Amiruddin[1,2], Samsu Arif[1*], Muhammad Alimuddin Hamzah Assegaf[1], Sakka[1], Fahruddin[1]

[1] Department of Geophysics, Faculty of Mathematics and Natural Sciences, Hasanuddin University, Makassar 90245, Indonesia
[2] Laboratory of Geoinformatics, Hasanuddin University, Makassar 90245, Indonesia
* Corresponding author's e-mail: samsu_arif@unhas.ac.id

## ABSTRACT

This study aims to analyze flood susceptibility and evaluate the spatial exposure of settlement areas in Barru regency, Indonesia, using a geographic information system (GIS) and a random forest approach. Environmental variables, including elevation, slope, soil type, rainfall, land cover, and river buffer, were integrated into the model. Flood susceptibility was expressed as probability values ranging from 0 to 1 and subsequently classified into low, moderate, and high categories for interpretation. The results show that low susceptibility dominates the study area (67.51%), followed by moderate (15.47%) and high susceptibility (17.02%). Model evaluation indicates stable performance, with an accuracy of approximately 0.86 and consistent results across validation schemes. Variable importance analysis identifies elevation as the most influential factor, followed by slope and soil type, highlighting the dominant role of topographic characteristics. Spatial overlay analysis reveals that approximately 72.63% of settlement areas are located within high susceptibility zones, indicating substantial exposure. These findings emphasize the importance of integrating flood susceptibility assessment into spatial planning to support susceptibility-informed and more sustainable settlement development in hazard-prone areas.

**Keywords:** flood susceptibility, machine learning, spatial analysis, settlement exposure, environmental factors, Barru regency.

## INTRODUCTION

Environmental systems are complex and dynamic, shaped by interactions between biotic and abiotic components that regulate key ecological functions and maintain ecosystem stability (Chamard et al., 2024). However, these systems are continuously influenced by natural processes and human activities, which may affect their stability. Changes in environmental conditions, such as climate variability, land transformation, and anthropogenic pressures, can disrupt ecological equilibrium and generate various environmental challenges (Chen et al., 2025; Fayshal, 2024). As these pressures increase, many regions worldwide are experiencing heightened vulnerability to environmental degradation and hazards (Xie et al., 2024). Therefore, understanding these dynamics is essential for sustainable environmental management and disaster risk reduction (Ogunbode et al., 2025).

One of the clearest manifestations of environmental change is the rapid expansion of settlements. Population growth and socio-economic development have increased demand for residential land, leading to the conversion of natural landscapes into built-up areas (Bikis et al., 2025). These transformations alter hydrological processes, particularly infiltration and runoff patterns (Agumagu et al., 2025). In many cases, settlement development occurs without adequate consideration of environmental constraints or hazard susceptibility, increasing community exposure to flood hazards (Badshah et al., 2024). Consequently, the spatial distribution

and planning of settlements play a critical role in determining vulnerability to natural hazards. Among these hazards, floods are among the most frequent and destructive, significantly impacting settlements, infrastructure, agriculture, and ecosystems (Feizbahr et al., 2025). Flood occurrence is controlled by climatic, hydrological, and geomorphological factors, while urban expansion and reduced natural infiltration further increase runoff and flood risk. Settlements located in low-lying areas or near rivers are particularly vulnerable (Zhang et al., 2025). Therefore, identifying flood-prone areas is essential to reduce disaster risk and support safer settlement planning (Fitriyati et al., 2024).

To better understand how flood susceptibility interacts with settlement development, it is important to examine these dynamics within a specific regional context. This study focuses on Barru regency, south Sulawesi province, Indonesia. The population growth rate reached 1.38% during 2020–2024, with a projected population of 195,388 in 2024 (BPS, 2025). Alongside rapid settlement expansion, flooding is one of the most frequent hazards in the region, influenced by tropical rainfall patterns, hydrological conditions, and low-lying terrain that increase susceptibility to inundation (Wulandari et al., 2025). These conditions highlight the importance of spatial analysis for understanding flood susceptibility and its implications for land-use planning (Oluwadare et al., 2025). In recent years, GIS-based spatial analysis has become a key tool for assessing environmental hazards and flood susceptibility (Bekalo et al., 2025). By integrating multiple spatial variables, GIS enables the evaluation of environmental influences on flood-prone areas (Amiruddin et al., 2026). Advances in computational methods have further promoted the use of machine learning for improving prediction accuracy, with the Random Forest algorithm widely applied due to its ability to model complex relationships and assess predictor importance (Danumah et al., 2026).

Although conventional GIS-based and multi-criteria evaluation (MCE) approaches have been widely used for flood susceptibility assessment and disaster mitigation (Ahmad, Ping, et al., 2025), they are limited by their reliance on predetermined parameter weights and simplified assumptions of environmental interactions (Efraimidou and Spiliotis, 2024; Khan et al., 2025). These limitations reduce their ability to capture complex, nonlinear relationships among climatic, hydrological, and topographical variables, which may affect model accuracy, particularly in dynamic environments (Chomani and Al-shrafany, 2025; Riaz and Mohiuddin, 2025). Moreover, previous studies often focus separately on hazard mapping or settlement exposure, without integrating both within a comprehensive spatial framework (Anastasia et al., 2021). This lack of integration, combined with the limitations of conventional methods, represents a critical gap in flood risk assessment. Addressing this gap requires data-driven approaches capable of modelling nonlinear relationships while simultaneously evaluating hazard and exposure. Therefore, this study applies a GIS-based random forest model to assess flood susceptibility and settlement exposure in Barru regency, providing more integrated and accurate insights to support spatial planning and flood hazard mitigation.

## MATERIALS AND METHODS

### Study area

Barru regency, located along the western coastal zone of south Sulawesi province, Indonesia (4°05′49″–4°47′35″ S, 119°35′00″–119°49′16″ E), serves as the study area. The regency covers approximately 1,198.9 km² with a 78 km coastline along the Makassar Strait and lies between Makassar and Parepare, about 100 km north of Makassar and 50 km south of Parepare City. Administratively, it comprises seven districts: Pujananting, Tanete Riaja, Tanete Rilau, Barru, Balusu, Soppeng Riaja, and Mallusetasi. Digital boundary data were obtained from the Geospatial Information Agency (BIG) in vector (shapefile) and raster (GeoTIFF,.tif) formats with WGS 84 coordinate system and are provided as supplementary materials (Figure 1). Climatic and hydrological characteristics, including rainfall variability, are key factors influencing flood occurrence in the study area.

### Data sources and preparation

This study used spatial and statistical datasets representing environmental and socio-demographic factors relevant to flood susceptibility analysis. The data included topographic, climatic, hydrological, land cover, soil, and settlement

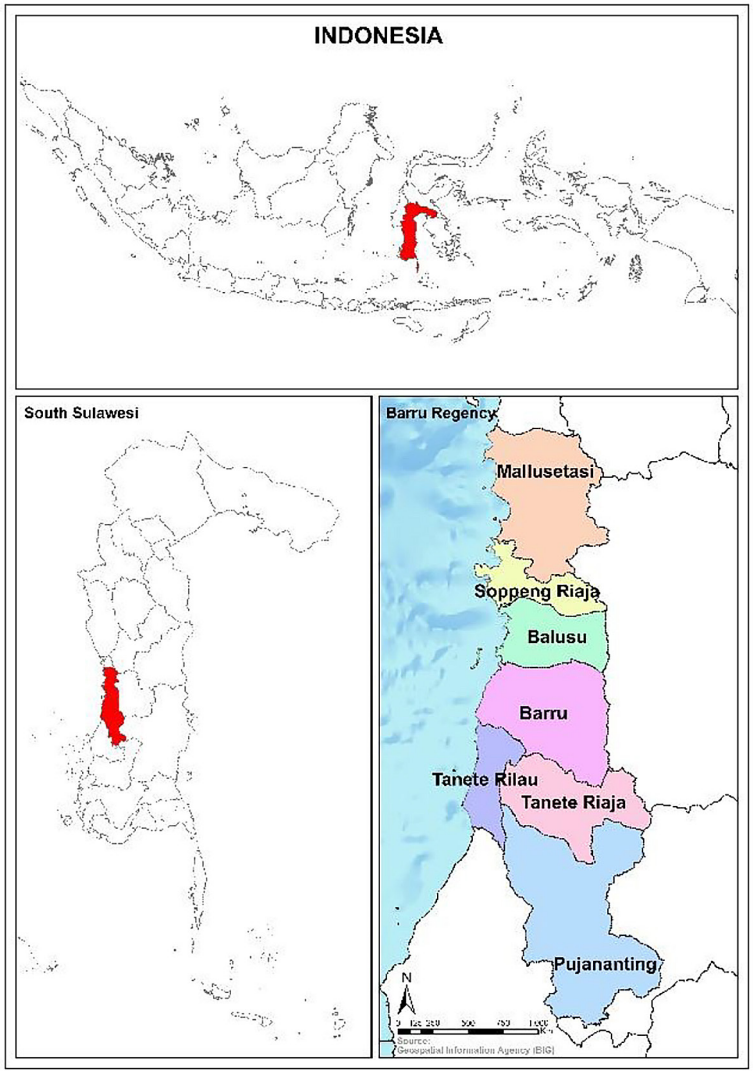


**Figure 1.** Location of the study area in Barru regency, south Sulawesi, Indonesia

information obtained from official and open-access sources. These datasets were used to characterize environmental conditions influencing flood occurrence and settlement distribution in Barru regency (Table 1). Prior to analysis, all datasets were preprocessed using ArcGIS 10.6 to ensure consistency. They were standardized to a common coordinate system and spatial resolution, with raster data resampled to 30 × 30 m and vector data converted to raster format. Preprocessing steps included reprojection, resampling, rasterization, and clipping based on the administrative boundary. The overall workflow is presented in Figure 2. A statistical summary of the rainfall dataset used in this study, including minimum, maximum, mean, and standard deviation values for the period 2015–2024, is presented in Table 2 to provide a descriptive overview of rainfall variability across the study area.

## Flood susceptibility parameters

This study utilized spatial and statistical datasets representing key environmental factors influencing flood susceptibility in Barru regency. Six environmental parameters were selected based on their direct influence on flood occurrence and settlement exposure (Ahmad et al., 2025; Singha et al., 2024). Elevation and slope were derived from the Digital Elevation Model Nasional (DEMNAS) to capture topographic variations that govern surface runoff and flood accumulation; areas with low elevation and gentle slopes are generally more prone to waterlogging (Jiang et al., 2025). Additionally, rainfall data, representing the annual average from 2015 to 2024, were obtained from CHIRPS, as precipitation intensity and distribution directly determine surface flow volume that can trigger flooding (Jawale and

**Table 1.** Spatial datasets used in this study

| Data | Description | Source |
|---|---|---|
| Population data | Population statistics representing demographic pressure on settlement development | Statistics of Barru Regency 2025 |
| Administrative boundary of Barru Regency | Regency and sub-district administrative boundaries | Geospatial Information Agency (BIG) https://tanahair.indonesia.go.id/ |
| DEMNAS (Digital Elevation Model Nasional) | Digital elevation model used to derive elevation and slope | Digital Elevation Model Nasional (DEMNAS) https://tanahair.indonesia.go.id/demnas |
| Rainfall data | Average annual rainfall (2015–2024) | CHIRPS https://www.chc.ucsb.edu/data/chirps |
| Land cover data | Land cover classification representing surface conditions | Esri Land Cover https://livingatlas.arcgis.com/landcover |
| River buffer | River buffer used to calculate distance-to-river parameter | Geospatial Information Agency (BIG) https://tanahair.indonesia.go.id/ |
| Soil type data | Soil classification related to hydrological characteristics | FAO/UNESCO Soil Map of the World https://www.fao.org |
| Settlement area | Spatial distribution of residential areas | Barru Regency Spatial Plan (RTRW) 2011–2031 |
| Spatial planning data (RTRW) | Land-use zoning regulations | Barru Regency Regulation No. 4 of 2012 |

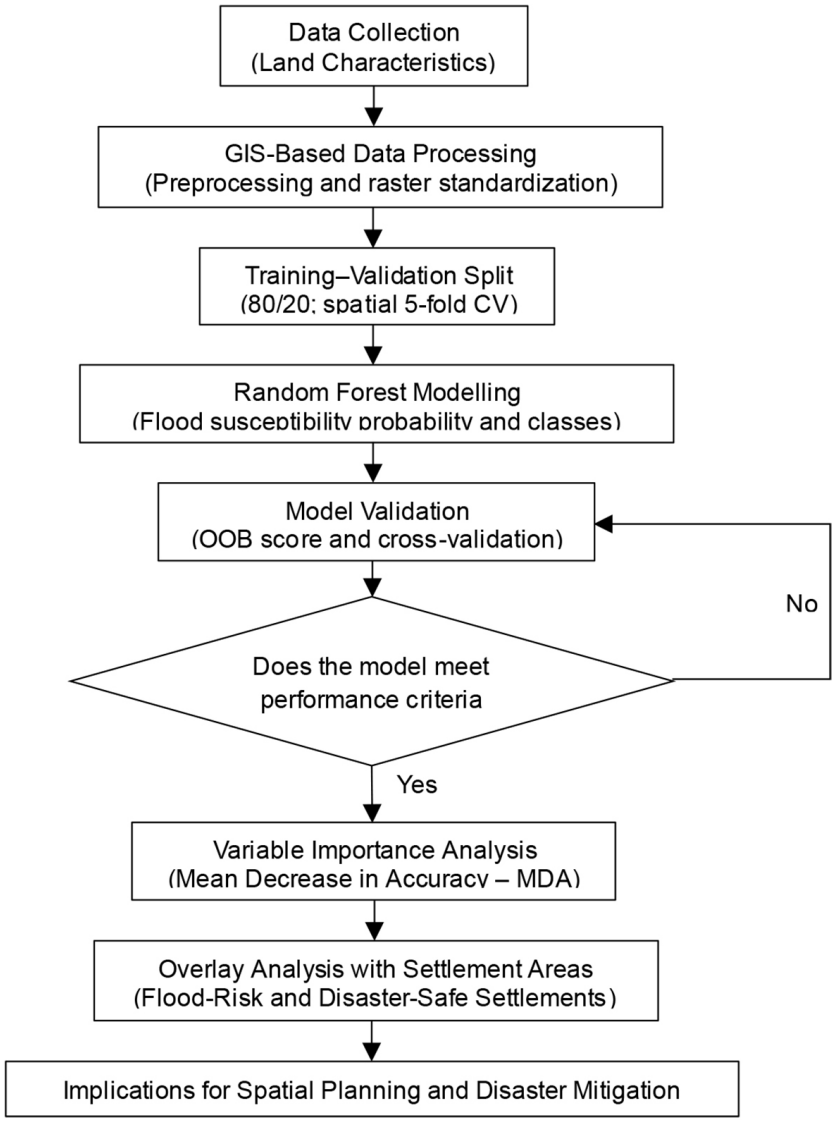


**Figure 2.** Research workflow of the study

**Table 2.** Statistical summary of rainfall data (2015–2024)

| Parameter | Value |
|---|---|
| Data source | CHIRPS |
| Period | 2015–2024 |
| Minimum rainfall | 2277.70 mm |
| Maximum rainfall | 2820.60 mm |
| Mean rainfall | 2587.50 mm |
| Standard deviation | 95.16 mm |

Thube, 2025). Soil type, sourced from the FAO/UNESCO Soil Map of the World, was included because soil characteristics control infiltration, water retention, and surface runoff rates; for instance, clayey soils tend to increase waterlogging risk (Rupngam and Messiga, 2024). Land cover, derived from Esri Land Cover datasets, was considered due to its influence on surface hydrology and runoff dynamics, as impervious surfaces and built-up areas reduce infiltration and accelerate runoff (Umukiza et al., 2024). River proximity, represented by Euclidean distance buffers from the local river network obtained from the Geospatial Information Agency (BIG), was used to quantify settlement exposure to fluvial flooding, since areas closer to rivers generally face higher flood risk (Alrifai et al., 2025). Finally, settlement area data, extracted from the Barru Regency Spatial Plan (RTRW) 2011–2031, were incorporated to identify vulnerable residential zones, enabling the analysis to assess both flood susceptibility and potential impacts (Table 3).

Training data for flood susceptibility modelling were generated using spatial sample points distributed across the study area. Sampling points representing flood-prone and non-flood areas were selected to ensure balanced spatial representation. The dataset was constructed using a stratified random sampling approach to ensure that variations in topography, land use, and flood susceptibility conditions were proportionally represented across the study area. The dependent variable (Y) was derived from the flood-related layer obtained from the INA-RISK platform developed by the National Disaster Management Agency (BNPB). This dataset was used as a reference proxy for identifying flood-prone and non-flood areas across the study area. The flood-related classes from the INA-RISK dataset were converted into binary labels, where flood-prone areas were assigned (label = 1) and non-flood areas were assigned (label = 0). These binary labels served as the training targets for the Random Forest model.

**Table 3.** Environmental parameters used for flood susceptibility modelling

| Parameter | Unit | Source |
|---|---|---|
| Slope | % | DEMNAS |
| Rainfall (2015–2024) | mm/year | CHIRPS |
| River buffer | m | BIG |
| Elevation | m | DEMNAS |
| Soil type | - | FAO/UNESCO Soil Map of the World |
| Land cover (2024) | - | Esri Land Cover |

Flood susceptibility modelling was performed using the random forest algorithm to analyze the relationship between environmental variables and flood occurrence, producing probability values that were subsequently classified into susceptibility levels.

## Random forest modelling

The random forest model was developed using Python 3.13.10 within the Anaconda environment, employing scikit-learn (v1.7.2) along with NumPy, pandas, and GeoPandas for spatial data processing. Input data, including environmental parameters and sampling points, were maintained in shapefile (SHP) format. Flood-prone and non-flood points (250 per class per district) were used to ensure balanced representation, with flood-prone areas assigned label 1 and non-flood areas assigned label 0. Numerical variables were used directly, while categorical variables (soil type and land cover) were encoded using OneHotEncoder.

The dataset was divided into training and testing subsets using two data partition schemes, namely 80% training and 20% testing, and 70% training and 30% testing. The splitting process was performed using a stratified random sampling approach to preserve class balance, with a fixed random seed (random_state = 42) to ensure reproducibility of the results. The use of multiple data partitions supports the assessment of model robustness, while detailed performance comparisons are presented in the model evaluation section.

The random forest model was configured with 100 decision trees (n_estimators = 100), a maximum tree depth of 10 (max_depth = 10), and a random subset of predictor variables determined using max_features = sqrt. The Gini index was used as the splitting criterion, and

final predictions were obtained through majority voting across trees (Park et al., 2019; Sun et al., 2020). Parameter tuning was conducted by testing different values of n_estimators (50, 100, 200) and max_depth (5, 10, 15) to obtain an optimal configuration. The selected configuration provided a balance between predictive accuracy and computational efficiency. The trained random forest model was subsequently applied to generate spatially explicit flood susceptibility probabilities across the study area based on the selected environmental parameters (Lange et al., 2025; Magalhães et al., 2024).

## Model validation

Model validation was conducted to evaluate the predictive performance and robustness of the Random Forest model. The dataset was divided into training and testing subsets using stratified random sampling to preserve class balance, employing two partition schemes of 80/20 and 70/30.

In addition to the train–test split, a 5-fold cross-validation approach was applied to further assess model stability. In this approach, the dataset was randomly partitioned into five folds of approximately equal size, where the model was iteratively trained on four folds and validated on the remaining fold until each fold had been used as validation data (Park et al., 2019; Riaz and Mohiuddin, 2025). To complement external validation, out-of-bag (OOB) scoring was also used as an internal validation method inherent to the Random Forest algorithm. This method estimates model performance using bootstrap samples during training, allowing an additional unbiased evaluation without requiring a separate validation dataset.

For reproducibility, a fixed random seed (random_state = 42) was applied during data splitting and model training. Model performance was evaluated using accuracy, precision, recall, and F1-score derived from the confusion matrix (Agboola et al., 2024; Markoulidakis and Markoulidakis, 2024; Sujon et al., 2025). The evaluation metrics are defined as follows:

$$Accuracy = \frac{TP + TN}{TP + TN + FP + FN} \quad (1)$$

$$Precision = \frac{TP}{TP + FP} \quad (2)$$

$$Recall = \frac{TP}{TP + FN} \quad (3)$$

$$F1 = 2 \times \frac{Precision \times Recall}{Precision + Recall} \quad (4)$$

where: TP (true positive) represents correctly predicted flood-prone areas, TN (true negative) represents correctly predicted non-flood areas, FP (false positive) represents non-flood areas incorrectly predicted as flood-prone, while FN (false negative) represents flood-prone areas incorrectly predicted as non-flood areas.

## Variable importance analysis

The relative importance of the predictor variables was evaluated using the mean decrease in accuracy (MDA) metric derived from the permutation importance procedure within the Random Forest model. This method evaluates the contribution of each predictor by measuring the decrease in model accuracy after random permutation of its values. A larger decrease in accuracy indicates that the variable plays a more important role in the model's predictive performance. Higher MDA values indicate greater variable importance in determining flood susceptibility (Debeer and Strobl, 2020; Hooker et al., 2021; Wies et al., 2023). In this study, permutation importance was computed using 10 random permutations (n_repeats = 10) with a fixed random seed (random_state = 42), consistent with the model configuration, to ensure reproducibility of the results.

## Flood susceptibility mapping and settlement overlay analysis

The flood susceptibility probability values generated by the random forest model were transformed into a flood susceptibility map covering the entire study area. The model output consists of continuous flood susceptibility probability based on environmental parameters. To facilitate spatial interpretation, the probability values were classified into three susceptibility levels: class 1 (low susceptibility), class 2 (moderate susceptibility), and class 3 (high susceptibility). The classification was performed using fixed threshold values, where probabilities ≤ 0.33 were classified as low susceptibility, values between 0.33 and 0.66 as moderate susceptibility, and values > 0.66 as high susceptibility. Subsequently, the flood susceptibility map was

overlaid with settlement areas derived from the Barru regency spatial plan (RTRW). The overlay analysis was conducted in a Python-based GIS environment using raster–vector integration techniques (GeoPandas and Rasterio). Specifically, settlement polygons were used to mask the raster-based flood susceptibility map using a geometry masking approach, allowing the extraction of susceptibility values within settlement areas. Through this process, settlement areas were categorized into low, moderate, and high susceptibility zones based on the underlying raster classification. This approach enables a spatially explicit assessment of settlement exposure to flood susceptibility. The results of this analysis were further used to evaluate settlement conditions and support spatial planning and disaster mitigation efforts in Barru regency.

## RESULTS

### Spatial distribution of flood susceptibility parameters

Figure 3 illustrates the spatial distribution of environmental parameters used in flood susceptibility modelling. Slope (Figure 3a) shows that low-gradient areas are mainly located in central to coastal regions, which may enhance surface water accumulation. Rainfall (Figure 3b) is relatively uniform with minor spatial variation, indicating limited spatial differentiation in precipitation patterns across the study area. Soil type (Figure 3c) exhibits heterogeneity, reflecting variations in infiltration capacity and hydrological response. Land cover (Figure 3d) is dominated by forest areas, while agricultural land and settlements are primarily concentrated in lowland regions. This pattern

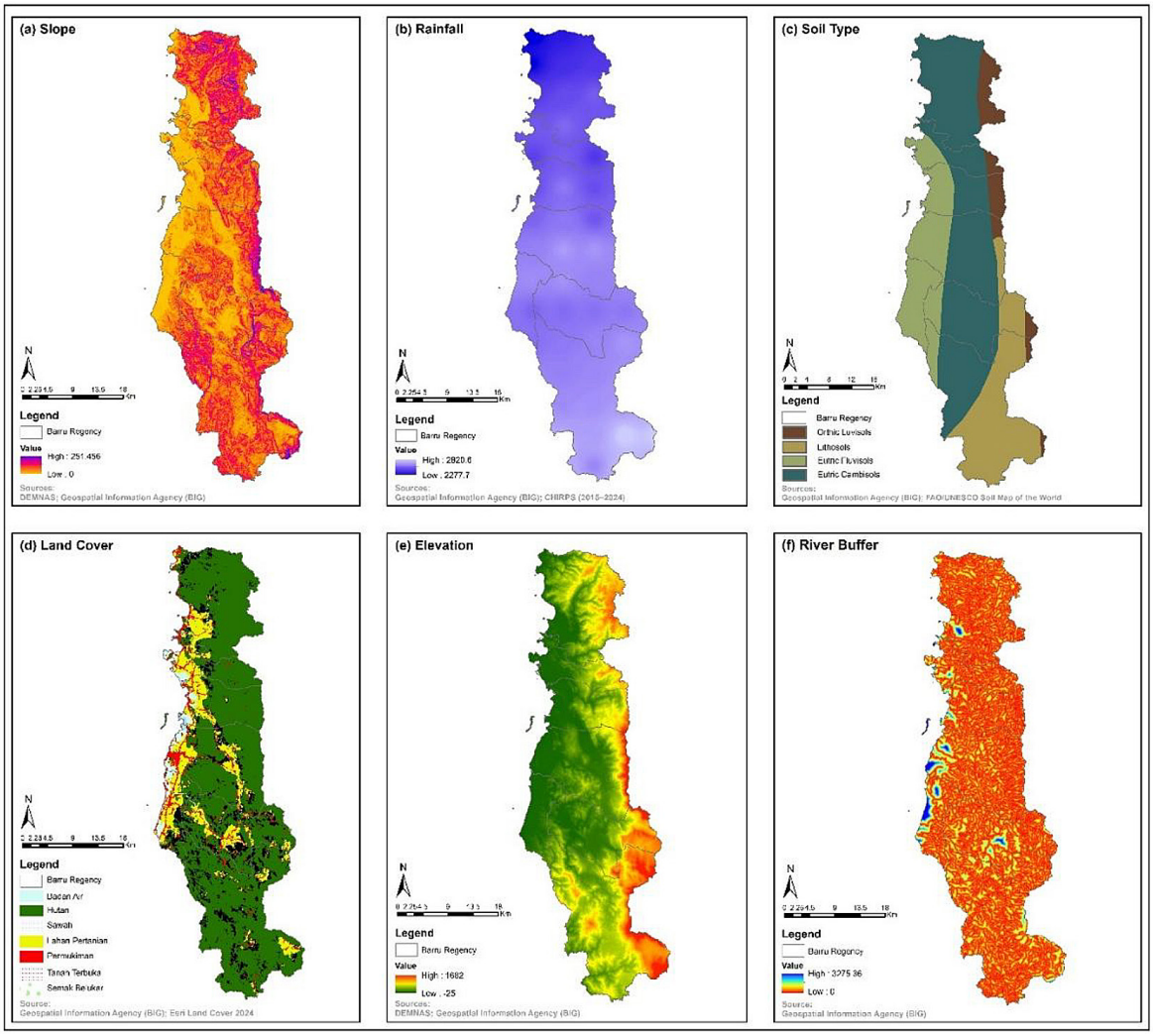


**Figure 3.** Spatial distribution of environmental parameters used for flood susceptibility modelling in Barru regency: (a) slope, (b) rainfall, (c) soil type, (d) land cover, (e) elevation, and (f) river buffer

corresponds with elevation (Figure 3e), where lower elevations are associated with increased potential for water accumulation. The river buffer (Figure 3f) highlights areas in close proximity to river networks, which are more susceptible to flooding due to potential overflow. Overall, the spatial patterns indicate that low-elevation, low-slope areas located near river networks and dominated by certain land cover types are more likely to contribute to higher flood susceptibility. These spatial relationships, as evidenced in Figure 3, provide the basis for the subsequent modelling process using the random forest algorithm.

## Flood susceptibility mapping

The random forest model produced a flood susceptibility map with probability values ranging from 0 to 1, representing the likelihood of flood occurrence at each pixel across Barru regency. The spatial distribution of these probability values is presented in Figure 4a. Areas with high probability values approaching 1 are primarily concentrated in lowland regions, coastal zones, and areas adjacent to major river networks, characterized by low elevation and high runoff potential. In contrast, regions with higher elevation and steeper slopes tend to exhibit lower probability values approaching 0, indicating lower flood susceptibility. To improve interpretability, the continuous probability values were subsequently classified into three categories: low, moderate, and high susceptibility using fixed threshold values (≤0.33; 0.33–0.66; >0.66). This classification was applied as a post-modeling step and did not influence the Random Forest training process. The resulting map is shown in Figure 4b, where high-susceptibility zones are mainly associated with lowland areas, coastal plains, and river corridors. Moderate susceptibility is generally observed in transitional zones between lowlands and elevated terrain, while low-susceptibility areas are predominantly located in hilly to mountainous regions.

Based on Table 4, low susceptibility dominates the study area, covering 67.51% (119,890.62 ha), followed by moderate susceptibility at 15.47% and high susceptibility at 17.02%. At the sub-district level, Mallusetasi and Pujananting are largely characterized by low-susceptibility conditions, accounting for 76.57% and 75.34% of their respective areas. In contrast, Tanete Rilau shows a different pattern, where high susceptibility constitutes the largest proportion (45.14%). Barru and Balusu show a relatively balanced distribution between low and high susceptibility classes, whereas Soppeng Riaja and Tanete Riaja remain predominantly low-susceptibility despite the presence of localized high-susceptibility zones. The reliability of the susceptibility map is supported by the consistent validation results presented in Table 5 and Table 6.

## Model performance and validation

Model performance was evaluated using two data partition schemes (80/20 and 70/30), with results summarized in Table 5. The model achieved comparable overall accuracy values of 0.8629 and 0.8619, respectively, indicating stable performance across different data splits. Other evaluation metrics, including weighted precision, weighted recall, and weighted F1-score, also show consistent values of approximately 0.86, suggesting balanced classification performance between flood-prone and non-flood classes.

The OOB scores of 0.8632 and 0.8629 further confirm the reliability of the model's internal validation. The close agreement between OOB scores

**Table 4.** Areal distribution of flood susceptibility classes by sub-district in Barru regency

| Sub-district | Sub-district area (ha) | Low susceptibility | | Moderate susceptibility | | High susceptibility | |
|---|---|---|---|---|---|---|---|
| | | ha | % | ha | % | ha | % |
| Barru | 20,436.57 | 12,461.67 | 61.01 | 3,387.69 | 16.58 | 4,587.21 | 22.41 |
| Tanete Rilau | 6,941.97 | 2,867.31 | 41.3 | 941.04 | 13.56 | 3,133.62 | 45.14 |
| Soppeng Riaja | 7,860.24 | 4,373.55 | 55.66 | 965.52 | 12.28 | 2,521.17 | 32.06 |
| Balusu | 10,916.37 | 6,723.72 | 61.6 | 1,404.99 | 12.87 | 2,787.66 | 25.53 |
| Mallusetasi | 22,692.15 | 17,373.87 | 76.57 | 2,423.34 | 10.68 | 2,894.94 | 12.75 |
| Tanete Riaja | 15,997.41 | 10,727.64 | 67.06 | 2,944.71 | 18.41 | 2,325.06 | 14.53 |
| Pujananting | 35,045.91 | 26,398.17 | 75.34 | 6,488.01 | 18.51 | 2,159.73 | 6.16 |
| Total Area | 119,890.62 | 80,925.93 | 67.51 | 18,555.30 | 15.47 | 20,409.39 | 17.02 |

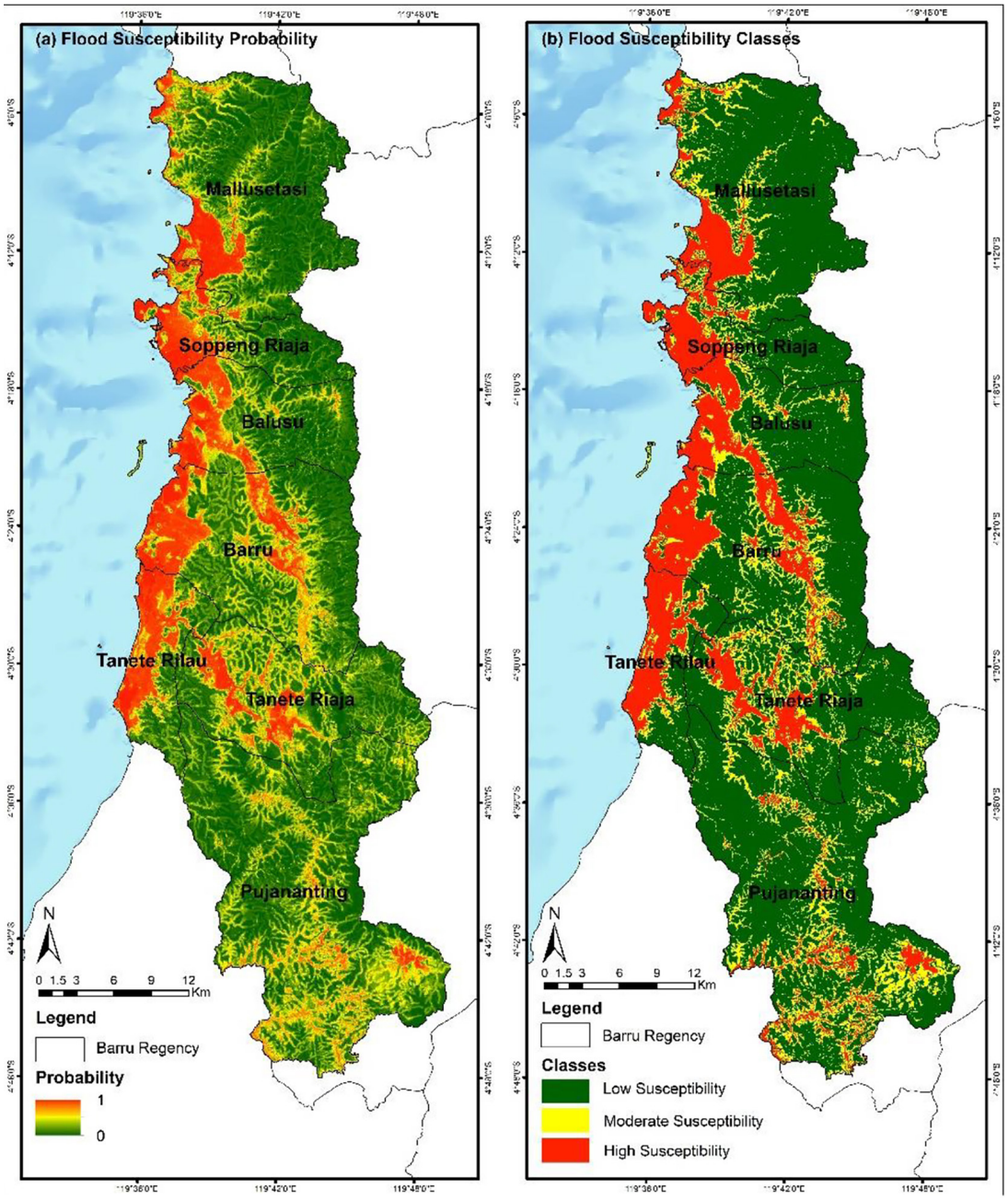


**Figure 4.** Flood susceptibility in Barru regency: (a) flood susceptibility probability; (b) flood susceptibility classes

**Table 5.** Performance evaluation metrics of the random forest model under different data partition schemes

| Evaluation metric | 80/20 scheme | 70/30 scheme |
|---|---|---|
| Accuracy | 0.8629 | 0.8619 |
| Precision (weighted) | 0.8638 | 0.863 |
| Recall (weighted) | 0.8629 | 0.8619 |
| F1-score (weighted) | 0.8628 | 0.8618 |
| Out-of-bag (OOB) score | 0.8632 | 0.8629 |
| Cross-validation mean | 0.8209 | 0.8209 |
| Cross-validation std | 0.102 | 0.102 |

and test accuracy indicates that the model does not suffer from overfitting and maintains good generalization capability. Additionally, 5-fold cross-validation yielded a mean accuracy of 0.8209 with a standard deviation of 0.102, as presented in Table 5. The fold-by-fold accuracy values are detailed in Table 6, providing transparent evidence of model performance variability across different subsets of the data. Most folds show high accuracy values above 0.85 (Fold 1, 2, 4, and 5), while one fold exhibits a lower accuracy (0.617). This variation

**Table 6.** 5-fold cross-validation accuracy results

| Fold | Accuracy |
|---|---|
| 1 | 0.874286 |
| 2 | 0.877143 |
| 3 | 0.617143 |
| 4 | 0.875714 |
| 5 | 0.86 |

suggests that model performance is influenced by spatial heterogeneity in environmental conditions and the distribution of flood and non-flood samples within the dataset.

Despite this variability, the overall consistency between multiple validation approaches – train–test split, OOB estimation, and cross-validation – demonstrates that the Random Forest model is robust and reliable. The inclusion of detailed fold-level results (Table 6) and multiple evaluation metrics (Table 5) provides empirical support for the validity of the modelling results, ensuring transparency and reproducibility in accordance with scientific research standards.

## Variable importance analysis

Variable importance analysis was conducted to quantify the relative contribution of each environmental predictor in the random forest model using the mean decrease in accuracy (MDA) metric derived from permutation importance. The results are presented in Table 7 and visually illustrated in Figure 5, providing both numerical and graphical evidence of the relative importance of each variable.

Elevation emerged as the most influential predictor, with an MDA value of 0.3353, which is substantially higher than all other variables. This dominant contribution, as clearly shown in Figure 5, indicates that topographic conditions play a critical role in controlling flood susceptibility. Low-lying areas tend to accumulate surface water more easily, making them more prone to flooding. Slope and soil type also show considerable contributions, with MDA values of 0.0881 and 0.0701, respectively (Table 7). These variables influence runoff dynamics and infiltration capacity, thereby affecting flood generation processes. River buffer distance (MDA = 0.0552) and land cover (MDA = 0.0536) exhibit moderate importance, as they represent proximity to water sources and surface characteristics that regulate hydrological responses. Rainfall shows the lowest contribution among all predictors, with an MDA value of 0.0430. This relatively lower importance is consistent with the spatial distribution of rainfall presented in Figure 3, which indicates limited variability across the study area. As a result, rainfall contributes less to distinguishing flood-prone and non-flood areas compared to topographic and land surface variables.

Overall, the consistency between the numerical results (Table 7) and the graphical representation (Figure 6) provides strong empirical evidence that topographic and land surface characteristics, particularly elevation, are the dominant controlling factors in flood susceptibility patterns in Barru regency. These findings are consistent

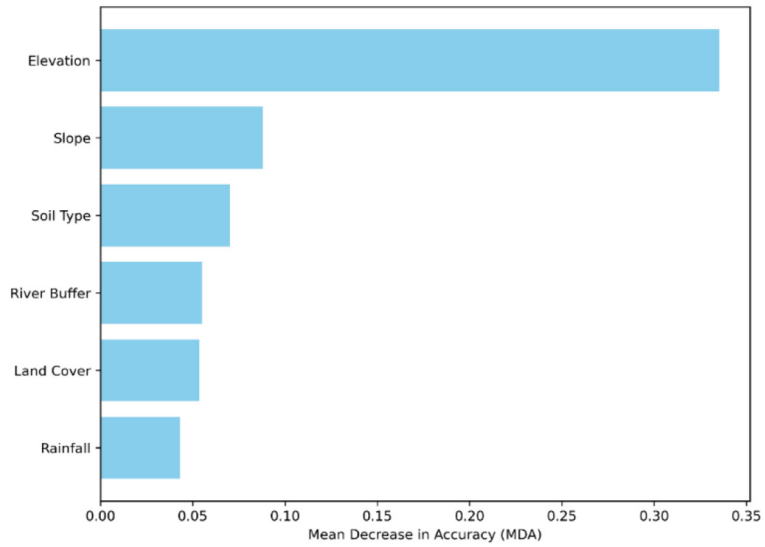


**Figure 5.** Variable importance (MDA) from the random forest model, with elevation as the dominant predictor

**Table 7.** Variable importance based on mean decrease accuracy (MDA) in the random forest model

| Rank | Predictor | MDA |
|---|---|---|
| 1 | Elevation | 0.335286 |
| 2 | Slope | 0.088107 |
| 3 | Soil type | 0.070107 |
| 4 | River buffer | 0.055179 |
| 5 | Land cover | 0.053643 |
| 6 | Rainfall | 0.043036 |

with fundamental hydrological principles, further supporting the robustness and interpretability of the model.

## Flood susceptibility and settlement overlay analysis

The spatial distribution of settlement areas in Barru regency derived from the Regional Spatial Plan is presented in Figure 6. Settlements are predominantly distributed along the western coastal zone, forming a linear pattern that follows the coastline. This pattern reflects the tendency of development to concentrate in accessible lowland areas. In addition to coastal concentrations, several scattered settlement clusters are observed inland, particularly in Barru, Tanete Rilau, and Tanete Riaja sub-districts, generally following local road networks and valley systems. In contrast, the northern and southern parts of the study area, especially in Mallusetasi and Pujananting, exhibit relatively limited settlement coverage, indicating lower development intensity.

The quantitative distribution of settlement areas is summarized in Table 8, showing that Barru sub-district accounts for the largest proportion of settlements (33.66%), followed by Tanete Rilau (20.28%) and Tanete Riaja (12.16%), while Pujananting has the smallest share (5.67%). Overall, this pattern indicates that settlement development is unevenly distributed and strongly concentrated in central and coastal lowland areas. This spatial configuration provides an important baseline for assessing the interaction between settlement distribution and flood susceptibility. The overlay of the flood susceptibility map and settlement data was conducted to evaluate settlement exposure to high-susceptibility areas. The spatial distribution of settlement exposure is presented in Figure 7, which clearly shows that a large proportion of settlements is located within high susceptibility zones (red areas), particularly in coastal plains and

**Table 8.** Areal extent of settlement areas by sub-district in Barru regency

| Sub-district | Area (ha) | Percentage (%) |
|---|---|---|
| Barru | 1211.49 | 33.66 |
| Tanete Rilau | 730.08 | 20.28 |
| Tanete Riaja | 437.58 | 12.16 |
| Soppeng Riaja | 362.70 | 10.08 |
| Mallusetasi | 344.07 | 9.56 |
| Balusu | 308.97 | 8.59 |
| Pujananting | 204.21 | 5.67 |
| Total | 3599.10 | 100.00 |

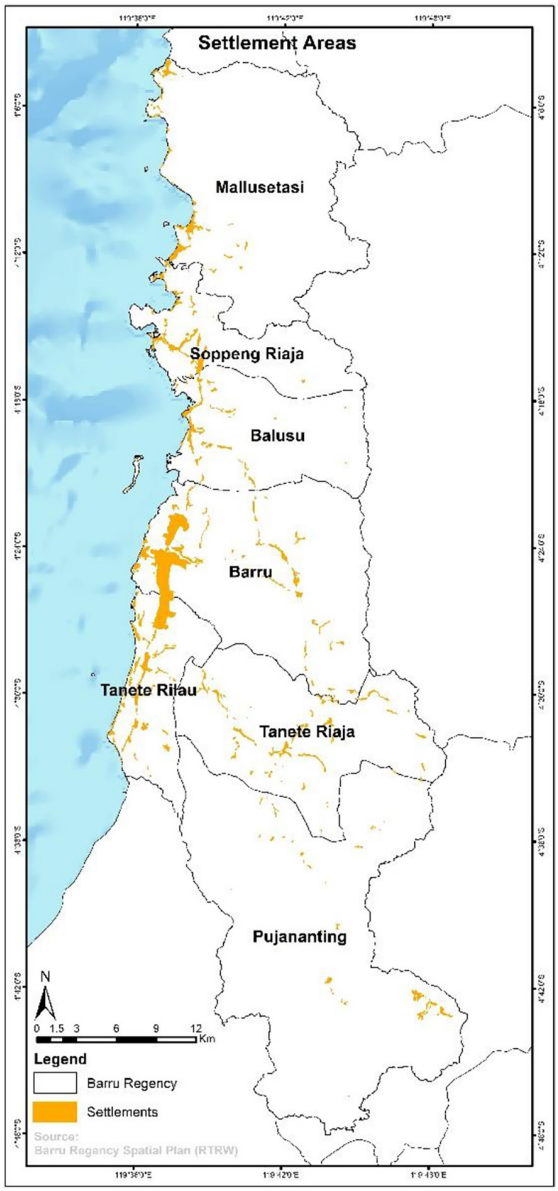


**Figure 6.** Spatial distribution of settlement areas derived from the Barru regency spatial plan

along river corridors. Moderate (yellow) and low (green) susceptibility zones are less dominant and more spatially fragmented. The quantitative results of settlement exposure are presented in Table 9. At the regency level, approximately 72.63% of the total settlement area (3,599.10 ha) is located within high susceptibility zones, while 17.95% and 9.42% fall within moderate and low susceptibility zones, respectively. This distribution indicates a strong concentration of settlements in hazard-prone areas. At the sub-district level, most areas are dominated by high flood susceptibility. Mallusetasi exhibits the highest proportion (94.51%), followed by Soppeng Riaja (82.85%), Tanete Rilau (78.57%), Balusu (78.42%), and Barru (75.62%). In contrast, Tanete Riaja and Pujananting show more varied patterns. Tanete Riaja, although still dominated by high susceptibility (46.26%), also contains significant proportions of low (30.87%) and moderate (22.87%) classes. Meanwhile, Pujananting is characterized by a relatively lower proportion of high susceptibility (26.27%), with moderate (42.31%) and low (31.42%) classes being more prominent.

Overall, the consistency between the spatial patterns shown in Figure 7 and the quantitative results in Table 9 provides strong empirical evidence of a spatial mismatch between settlement distribution and flood susceptibility. This indicates that a substantial proportion of settlements is located in high-susceptibility areas, highlighting critical implications for spatial planning, land-use management, and disaster risk reduction strategies in Barru regency.

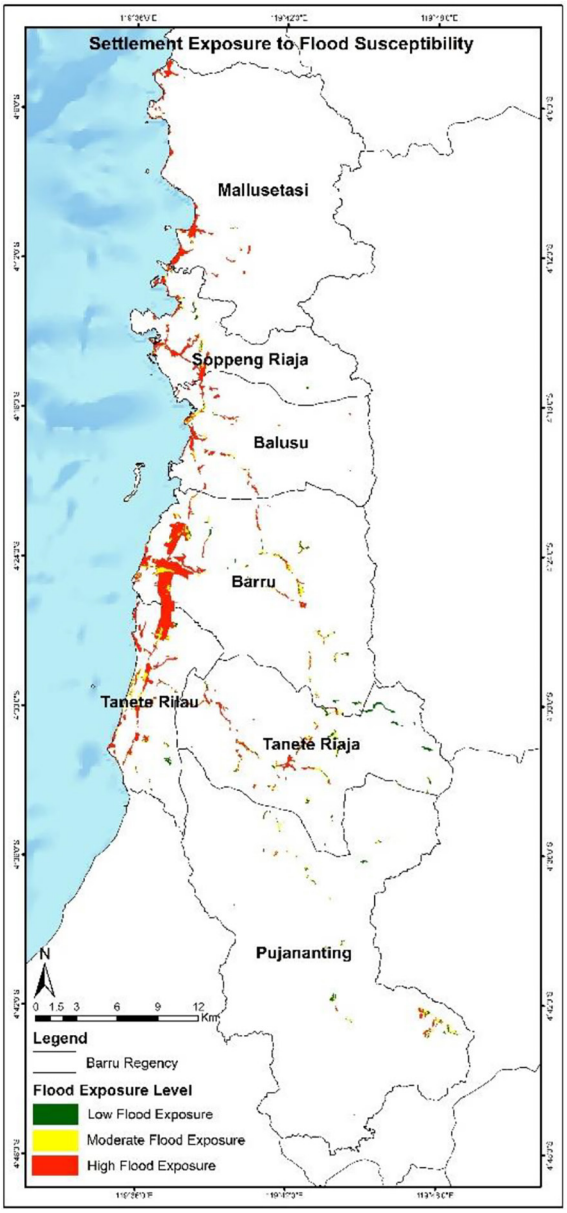


**Figure 7.** Spatial distribution of settlement exposure to flood susceptibility in Barru regency

## DISCUSSION

### Spatial pattern of settlement exposure to flood susceptibility

The spatial pattern of settlement exposure to flood susceptibility shows a clear concentration in the western coastal zone of the study area. In this study, exposure is defined as the spatial intersection between settlement areas and flood susceptibility probability, representing a combination of settlement extent and model-derived flood susceptibility. This configuration was obtained through an overlay analysis between settlement maps from the RTRW and the flood susceptibility probability map. The integrated results (Figure 7) indicate that a large proportion of settlements is located in high-susceptibility areas, consistent with previous studies showing that coastal regions are increasingly exposed to flooding due to dense settlement concentration and environmental changes (Aminur et al., 2024; Kunze and Strobl, 2024). The linear pattern of highly exposed settlements along the coastline highlights a strong spatial relationship between settlement expansion and flood-prone zones, particularly in low-lying coastal environments characterized by low elevation, proximity to water bodies, and limited drainage capacity (Zhou et al., 2024).

Quantitatively, approximately 72.63% of settlement areas fall within high-susceptibility zones, while only 9.42% are located in low-susceptibility

**Table 9.** Settlement exposure to flood susceptibility by Sub-district in Barru regency

| Sub-district | Total settlement (ha) | Low flood | | Moderate flood | | High flood | |
|---|---|---|---|---|---|---|---|
| | | (ha) | % | (ha) | % | (ha) | % |
| Barru | 1211.49 | 74.52 | 6.15 | 220.86 | 18.23 | 916.11 | 75.62 |
| Tanete Rilau | 730.08 | 30.33 | 4.15 | 126.09 | 17.27 | 573.66 | 78.57 |
| Tanete Riaja | 437.58 | 135.09 | 30.87 | 100.08 | 22.87 | 202.41 | 46.26 |
| Soppeng Riaja | 362.7 | 20.97 | 5.78 | 41.22 | 11.36 | 300.51 | 82.85 |
| Mallusetasi | 344.07 | 6.66 | 1.94 | 12.24 | 3.56 | 325.17 | 94.51 |
| Balusu | 308.97 | 7.47 | 2.42 | 59.22 | 19.17 | 242.28 | 78.42 |
| Pujananting | 204.21 | 64.17 | 31.42 | 86.4 | 42.31 | 53.64 | 26.27 |
| Total area | 3599.10 | 339.21 | 9.42 | 646.11 | 17.95 | 2613.78 | 72.63 |

areas, indicating that most settlements are exposed to elevated flood exposure. This distribution reflects not only environmental constraints but also socio-spatial drivers such as accessibility and proximity to economic activities, which tend to encourage development in coastal areas (Calcagni and Battisti, 2025; Fan et al., 2025). In contrast, inland areas exhibit a more heterogeneous exposure pattern due to greater topographic variability and localized environmental conditions (Liu et al., 2025).

## Influence of physical factors on flood exposure

The spatial distribution of settlement exposure to flood susceptibility may be further understood in relation to the physical characteristics of the study area, particularly geomorphological and hydrological conditions. Coastal and lowland regions are generally characterized by low elevation, gentle slopes, and limited natural drainage capacity, which facilitate water accumulation and increase the likelihood of inundation during high rainfall events (Al-ruzouq et al., 2024; He et al., 2025). The variable importance results from the Random Forest model further support this interpretation, where elevation and slope are identified as the most influential predictors.

In addition, the presence of river networks and their proximity to settlement areas play a significant role in shaping flood exposure. Areas located near rivers are more susceptible to flooding due to potential overflow when discharge exceeds channel capacity, particularly in downstream zones where river flow interacts with coastal processes (Gao et al., 2025; Yaseen, 2024). In contrast, areas with higher elevation and more complex topography tend to exhibit lower exposure, as these conditions promote more efficient runoff and drainage, thereby reducing water accumulation.

Although rainfall shows relatively low importance in the model, it does not mean it is insignificant in real-world flood processes. Its limited contribution is likely due to its relatively uniform spatial distribution across the study area. However, rainfall becomes more critical under temporal or seasonal conditions, especially during extreme events not captured by long-term averages. Therefore, while topographic and surface variables control spatial variability, rainfall remains an important triggering factor in flood events.

## Implications for spatial planning and flood risk reduction

The dominance of high settlement exposure to flood susceptibility (Figure 7) highlights important implications for spatial planning and disaster risk reduction in the study area. Many settlements, particularly along the western coastal zone, are located within high-susceptibility areas. When compared with settlement distribution (Figure 6), this pattern suggests that existing spatial planning, as reflected in the RTRW, may not fully integrate flood susceptibility considerations, with development more strongly influenced by accessibility, coastal proximity, and economic activities.

This interpretation is supported by the Random Forest variable importance results (Table 7), where elevation (MDA = 0.335) and slope (MDA = 0.088) are the most influential predictors. These values, derived from the Mean Decrease in Accuracy (MDA) metric, indicate that low-lying and gently sloping areas – where settlements are concentrated – have higher flood susceptibility (Peiris, 2024; Gawrysiak et al., 2024). The distribution

of settlements further confirms this imbalance, with 72.63% located in high-susceptibility zones and only 9.42% in low-susceptibility areas.

These findings provide a basis for more risk-informed spatial planning. Limiting settlement expansion in high-susceptibility zones, particularly in coastal areas, may be considered as one strategy, while optimizing land use in relatively safer inland areas may also support risk reduction. In this context, the integration of machine learning-based flood susceptibility modelling with spatial exposure analysis offers a data-driven framework for identifying priority areas for planning and mitigation. These approaches are not intended as prescriptive solutions, but rather as analytical support for adaptive and risk-based planning strategies (Chauhan et al., 2025; Kurugama et al., 2024).

From a future perspective, continued expansion of settlements into high-susceptibility zones – especially in coastal and river-adjacent areas – may significantly increase exposure and potential damage. Although rainfall shows lower importance in the model, its role may intensify under seasonal or extreme conditions, potentially exacerbating flood impacts in vulnerable areas. Therefore, integrating flood susceptibility information into spatial planning frameworks is essential to support more sustainable and risk-sensitive development.

## CONCLUSIONS

This study demonstrates that flood susceptibility in Barru regency exhibits clear spatial variability influenced by environmental conditions, as analysed using a random forest-based approach. The results indicate that low susceptibility dominates the region (67.51%), followed by moderate (15.47%) and high susceptibility (17.02%). However, overlay analysis reveals that a large proportion of settlement areas (72.63%) are located within high susceptibility zones, indicating a high level of exposure. The spatial pattern further shows that settlements are predominantly concentrated in lowland and coastal areas, which are more prone to flooding due to topographic and hydrological conditions. Among the influencing factors, elevation is identified as the most dominant, followed by slope and soil type, highlighting the key role of terrain characteristics in shaping flood susceptibility patterns. These findings emphasize the importance of integrating flood susceptibility assessments into spatial planning frameworks to support more susceptibility-informed and sustainable settlement development, particularly in reducing exposure in hazard-prone areas.

## Acknowledgments

The authors would like to express their sincere gratitude to all institutions and data providers that supported this research. Appreciation is extended to the Badan Informasi Geospasial for providing DEMNAS data, as well as to other relevant agencies that made spatial and environmental datasets accessible for this study. The authors also gratefully acknowledge the Department of Geophysics, particularly the Geoinformatics Laboratory Universitas Hasanuddin, for providing academic support, research facilities, and technical assistance during the data collection and analysis stages. Finally, the authors are grateful to the anonymous reviewers for their constructive comments and suggestions that helped improve the quality of this study.

## REFERENCES

1. Agboola, G., Hashemi, L., Elbayoumi, T., Thompson, G. (2024). Ecological informatics optimizing landslide susceptibility mapping using machine learning and geospatial techniques. *Ecological Informatics*, *81*. https://doi.org/10.1016/j.ecoinf.2024.102583
2. Agumagu, O. O., Marchant, R., Stringer, L. C. (2025). Land use and land cover change dynamics in the Niger Delta Region of Nigeria from 1986 to 2024. *Land*, *14*. https://doi.org/10.3390/land14040765
3. Ahmad, I., Farooq, R., Ashraf, M., Waseem, M., Shangguan, D. (2025). Improving flood hazard susceptibility assessment by integrating hydrodynamic modeling with remote sensing and ensemble machine learning. *Natural Hazards*, *121*. https://doi.org/10.1007/s11069-025-07109-2
4. Ahmad, I., Ping, W., Ullah, S., Faqeih, K. Y., Alamri, S. M., Alamery, E. R., Abdulaziz, A., Abalkhail, A. A. A., Jan, H. M. B. (2025). Spatiotemporal mapping of urban flood susceptibility: A Multi-criteria GIS-based assessment in Nangarhar, Afghanistan. *Land*, *14*. https://doi.org/10.3390/ land14122376
5. Al-ruzouq, R., Shanableh, A., Jena, R., Barakat, M., Gibril, A., Atalla, N., Lamghari, F. (2024). Geoscience Frontiers Flood susceptibility mapping using a novel integration of multi-temporal

sentinel-1 data and eXtreme deep learning model. *Geoscience Frontiers*, *15*. https://doi.org/10.1016/j.gsf.2024.101780

6. Alrifai, M. H., Kafy, A. Al, Altuwaijri, H. A. (2025). Quantitative assessment of flood risk through multi parameter morphometric analysis and GeoAI : A GIS-based study of Wadi Ranuna Basin in Saudi Arabia. *Water*, *17*. https://doi.org/10.3390/w17142108
7. Aminur, M., Shah, R., Wang, X. (2024). International Journal of Disaster Risk Reduction Assessing social-ecological vulnerability and risk to coastal flooding : A case study for Prince Edward Island, Canada. *International Journal of Disaster Risk Reduction*, *106*. https://doi.org/10.1016/j.ijdrr.2024.104450
8. Amiruddin, H. B., Arif, S., Sakka. (2026). Geospatial analysis of land degradation and settlement in Barru Regency: Implications for sustainable land management. *Journal of Degraded and Mining Lands Management*, *13*(1). https://doi.org/10.15243/jdmlm.2026.131.9081
9. Anastasia, S., Alimuddin, I., Arifin, F. (2021). Land suitability analysis for urban development using multihazard map in mamuju district, West Sulawesi province, Indonesia Land suitability analysis for urban development using multi- hazard map in mamuju district, West Sulawesi province, Indonesia. *Earth and Environmental Science*. https://doi.org/10.1088/1755-1315/921/1/012023
10. Badshah, M. T., Hussain, K., Rehman, A. U., Mehmood, K., Muhammad, B., Wiarta, R., Silamon, R. F., Khan, M. A., Meng, J. (2024). The role of random forest and Markov chain models in understanding metropolitan urban growth trajectory. *Frontiers in Forests and Global Change*, *7*, 1–17. https://doi.org/10.3389/ffgc.2024.1345047
11. Bekalo, J. D., Bojer, A. K., Debelee, T. G., Al-Quraishi, A. M. F., Negera, W. G., Gebissa, K. W., Nadarajah, S., Woldesillasie, F. F. (2025). Spatial modeling of flood hazard in addis ababa using geographic information system (GIS) and information gain ratio (IGR) method. *Journal of Flood Risk Management*, *18*. https://doi.org/10.1111/jfr3.70124
12. Bikis, A., Engdaw, M., Pandey, D., Pandey, B. K. (2025). The impact of urbanization on land use land cover change using geographic information system and remote sensing : a case of Mizan Aman City Southwest Ethiopia. *Scientific Reports*, *15*, 1–24. https://doi.org/10.1038/s41598-025-94189-6
13. BPS. (2025). *Kabupaten barru dalam angka 2025* (Vol. 17).
14. Calcagni, L., Battisti, A. (2025). Mapping opportunities for floating urban development along Italian waterfronts. *Sustainability*, *17*. https://doi.org/10.3390/su17052137
15. Chamard, J., Faticov, M., Blanchet, F. G., Chagnon, P.-L., Lapointe, I. L. (2024). Interplay of biotic and abiotic factors shapes tree seedling growth and root- associated microbial communities. *Communications Biology*, *7*. https://doi.org/10.1038/s42003-024-06042-7
16. Chauhan, V., Gupta, L., Dixit, J. (2025). Machine learning and GIS-based multi-hazard risk modeling for Uttarakhand : Integrating seismic, landslide, and flood susceptibility with socioeconomic vulnerability. *Environmental and Sustainability Indicators*, *26*. https://doi.org/10.1016/j.indic.2025.100664
17. Chen, K., Ma, L., Jiang, W., Wang, L., Wei, L., Zhang, H., Yang, R. (2025). Anthropogenic disturbance and climate change impacts on the suitable habitat of *Sphenomorphus incognitus* in China. *Ecology and Evolution*, *15*, 1–16. https://doi.org/10.1002/ece3.70848
18. Chomani, K., Al-shrafany, D. M. (2025). Innovative approaches to flood hazard assessment in semi-arid environments: A comparative analysis of multi-criteria and geospatial techniques. *Iraqi Geological Journal*, *58*. https://doi.org/10.46717/igj.2025.54.2A.6
19. Danumah, J. H., Ataba, W. A., Sokeng, J., Akpa, Y. L., Saley, M. B., Ogilvie, A. (2026). Assessing urban flood susceptibility using random forest machine learning and geospatial technologies: Application to the Bonoumin-Palmeraie Watershed, Abidjan ( C ô te d ' Ivoire ). *Water*, *18*, 1–19. https://doi.org/10.3390/w18030402
20. Debeer, D., Strobl, C. (2020). Conditional permutation importance revisited. *BMC Bioinformatics*, *21*, 1–30. https://doi.org/10.1186/s12859-020-03622-2
21. Efraimidou, E., Spiliotis, M. (2024). A GIS-based flood risk assessment using the decision-making trial and evaluation laboratory approach at a regional scale. *Environmental Processes*, *11*(9). https://doi.org/10.1007/s40710-024-00683-w
22. Fan, J., Liu, B., Lei, T., Sun, Y., Ma, Y., Guo, R., Chen, D., Zhou, K., Li, S., Gao, X. (2025). Exploring how economic level drives urban flood risk. *Nature Communications*, *16*. https://doi.org/10.1038/s41467-025-60267-6
23. Fayshal, M. A. (2024). Heliyon Current practices of plastic waste management, environmental impacts, and potential alternatives for reducing pollution and improving management. *Heliyon*, *10*. https://doi.org/10.1016/j.heliyon.2024.e40838
24. Feizbahr, M., Brake, N., Arbabkhah, H., Asli, H. H., Woods, K. (2025). Flood susceptibility mapping using machine learning and geospatial-Sentinel-1 SAR integration for enhanced early warning systems. *Remote Sensing*, *17*, 1–30. https://doi.org/10.3390/rs17203471
25. Fitriyati, N., Arifin, H. S., Kaswanto, R. L., Marimin. (2024). Enhancing land use planning through

integrating landscape analysis and flood inundation prediction Bekasi City' s in 2030. *Geomatics, Natural Hazards and Risk*, *15*(1). https://doi.org/10.1080/19475705.2024.2360623

26. Gao, H., Wang, Q., Zhou, Z., Wu, W., Wang, W., Li, Y., Hu, J., Li, P., Zhang, Y., Hu, W. (2025). Optimizing hydrodynamic regulation in coastal Plain River Networks in Eastern China: A MIKE11-based partitioned water allocation framework for flood control and water quality enhancement. *Water*, *17*. https://doi.org/10.3390/w17121829
27. He, F., Liu, S., Mo, X., Wang, Z. (2025). Interpretable flash flood susceptibility mapping in Yarlung Tsangpo River Basin using $H_2O$. *Scientific Reports*, *15*. https://doi.org/10.1038/s41598-024-84655-y
28. Hooker, G., Mentch, L., Zhou, S. (2021). Unrestricted permutation forces extrapolation : variable importance requires at least one more model, or there is no free variable importance. *Statistics and Computing*, *31*. https://doi.org/10.1007/s11222-021-10057-z
29. Jawale, P. S. J., Thube, A.. (2025). Rainfall-runoff modeling of urban floods using GIS and HEC-HMS. *MethodsX*, *15*. https://doi.org/10.1016/j.mex.2025.103437
30. Jiang, Y., Wang, L., Xie, T., Li, R., Wen, K., Liu, C., Hu, C. (2025). Study on the effect of underlying surface changes on runoff generation in the urbanized watershed. *Scientific Reports*, *15*. https://doi.org/10.1038/s41598-025-95295-1 1
31. Khan, N. A., Alzahrani, H., Bai, S., Hussain, M., Tayyab, M., Ullah, S., Ullah, K., Khalid, S. (2025). Flood risk assessment in the Swat river catchment through GIS-based multi-criteria decision analysis. *Frontiers in Environmental Science*, *13*. https://doi.org/10.3389/fenvs.2025.1567796
32. Kunze, S., Strobl, E. A. (2024). The global long-term effects of storm surge flooding on human settlements in coastal areas OPEN ACCESS The global long-term effects of storm surge flooding on human settlements in coastal areas. *Environmental Research*, *19*. https://doi.org/10.1088/1748-9326/ad18df
33. Kurugama, K. M., Kazama, S., Hiraga, Y., Samarasuriya, C. (2024). A comparative spatial analysis of flood susceptibility mapping using boosting machine learning algorithms in. *Journal of Flood Risk Management*, *17*. https://doi.org/10.1111/jfr3.12980
34. Lange, T. M., Gültas, M., Schmitt, A. O., Heinrich, F. (2025). optRF: Optimising random forest stability by determining the optimal number of trees. *BMC Bioinformatics*, 1–21. https://doi.org/10.1186/s12859-025-06097-1
35. Liu, J., Zhao, X., Chen, Y., Sun, H., Gu, Y., Xu, S. (2025). Geoscience Frontiers A novel flood conditioning factor based on topography for flood susceptibility modeling. *Geoscience Frontiers*, *16*. https://doi.org/10.1016/j.gsf.2024.101960
36. Magalhães, B., Bento, P., Pombo, J., Calado, M. do R., Mariano, S. (2024). Forest and optimal feature selection. *Energies*, *17*. https://doi.org/https://doi.org/ 10.3390/en17081926
37. Markoulidakis, I., Markoulidakis, G. (2024). Probabilistic confusion matrix: A novel method for machine learning algorithm generalized performance analysis. *Technologies*, *12*. https://doi.org/10.3390/technologies12070113
38. Ogunbode, T. O., Oyebamiji, V. O., Sanni, D. O., Akinwale, E. O., Akinluyi, F. O. (2025). Environmental impacts of urban growth and land use changes in tropical cities. *Frontiers in Sustainable Cities*, *6*, 1–11. https://doi.org/10.3389/frsc.2024.1481932
39. Oluwadare, T. S., Ribeiro, M. P., Chen, D., Ataabadi, M. B., Tabesh, S. H., Daomi, A. E. (2025). Applying machine learning algorithms for spatial modeling of flood susceptibility prediction over São Paulo Sub-Region. *Land*, *14*. https://doi.org/https://doi.org/10.3390/land14050985
40. Park, S., Hamm, S. Y., Kim, J. (2019). Performance evaluation of the GIS-based data-mining techniques decision tree, random forest, and rotation forest for landslide susceptibility modeling. *Sustainability (Switzerland)*, *11*(20). https://doi.org/10.3390/su11205659
41. Peiris, M. T. O. V. (2024). Assessment of urban resilience to floods: A spatial planning framework for cities. *Sustainability*, *16*. https://doi.org/10.3390/su16209117
42. Riaz, R., Mohiuddin, M. (2025). Application of GIS-based multi-criteria decision analysis of hydro-geomorphological factors for flash flood susceptibility mapping in Bangladesh. *Water Cycle*, *6*. https://doi.org/10.1016/j.watcyc.2024.09.003
43. Rupngam, T., Messiga, A. J. (2024). Unraveling the interactions between flooding dynamics and agricultural productivity in a changing climate. *Sustainability*, *16*. https://doi.org/10.3390/su16146141
44. Singha, C., Kumar, V., Quoc, R., Pham, B., Nguyen, D. C., Łupikasza, E. (2024). Integrating machine learning and geospatial data analysis for comprehensive flood hazard assessment. *Environmental Science and Pollution Research*, *31*. https://doi.org/10.1007/s11356-024-34286-7
45. Sujon, K. M., Hassan, R., Choi, K., Samad, M. A. (2025). Empirical evidence from advanced statistics, ML, and XAI for evaluating business predictive models. *Journal of Big Data*, *12*. https://doi.org/10.1186/s40537-025-01313-4
46. Sun, D., Wen, H., Wang, D., Xu, J. (2020). A random forest model of landslide susceptibility mapping based on hyperparameter optimization using Bayes algorithm. *Geomorphology*, *362*, 107201. https://doi.org/10.1016/j.geomorph.2020.107201

47. Umukiza, E., Abagale, F. K., Adongo, T. A. (2024). Characterization of landuse and landcover dynamics and their impact on runoff generation patterns in dam catchments of Northern Ghana. *Geocarto International*, *39*(1). https://doi.org/10.1080/10106049.2024.2335247
48. Gawrysiak L., Baran-Zgłobicka B., Zgłobicki W. (2024). Flash floods hazard to the settlement network versus land use planning (Lublin upland, east Poland). *Applied Sciences*, *14*. https://doi.org/10.3390/app14188425
49. Wies, C., Miltenberger, R., Grieser, G., Eimermacher, A. J. (2023). Exploring the variable importance in random forests under correlations: a general concept applied to donor organ quality in post - transplant survival. *BMC Medical Research Methodology*, *23*, 1–11. https://doi.org/10.1186/s12874-023-02023-2
50. Wulandari, S., Pratama, F., Andika, N., Wongso, P., Wijayasari, W., Rohmat, F. I. W. (2025). Identifying dominant river contributions to urban flooding: a scenario-based study of Makassar City. *Frontiers in Built Environment*, *11*, 1–15. https://doi.org/10.3389/fbuil.2025.1612416
51. Xie, H., Sun, Q., Song, W. (2024). Exploring the ecological effects of rural land use changes: A bibliometric overview. *Land*, *13*, 1–24. https://doi.org/10.3390/land13030303
52. Yaseen, Z. M. (2024). Flood hazards and susceptibility detection for Ganga river, Bihar state, India: Employment of remote sensing and statistical approaches. *Results in Engineering*, *21*. https://doi.org/10.1016/j.rineng.2023.101665
53. Zhang, Z., Wu, X., Chen, S., Jia, L., Wang, Q., Zhang, Z., Li, M., Jia, R., Lin, Q. (2025). Spatial pattern and driving mechanisms of settlements in the agro-pastoral ecotone of Northern China : A case study of Eastern Inner Mongolia. *Land*, *14*, 1–24. https://doi.org/10.3390/ land14061268
54. Zhou, K., Kong, F., Yin, H., Destouni, G., Meadows, M. E., Andersson, E., Chen, L., Chen, B., Li, Z., Su, J. (2024). Urban flood risk management needs nature-based solutions: a coupled social-ecological system perspective. *Npj Urban Sustainability*, *4*, 25. https://doi.org/10.1038/s42949-024-00162-z